Suppression of ferromagnetism in the $LaV_xCr_{1-x}Ge_3$ system

Xiao Lin,[1] Valentin Taufour,[1] Sergey L. Bud'ko,[1,2] and Paul C. Canfield[1,2]
[1]*Department of Physics and Astronomy, Iowa State University, Ames, Iowa 50011, USA*
[2]*Ames Laboratory, U.S. Department of Energy, Iowa State University, Ames, Iowa 50011, USA*
(Received 30 May 2013; revised manuscript received 25 July 2013; published 4 September 2013)

We report the synthesis of hexagonal $LaV_xCr_{1-x}Ge_3$ ($x = 0$–$0.21, 1.00$) single crystals and present a systematic study of this series by measurements of temperature- and field-dependent magnetic susceptibility, magnetization, resistivity, and specific heat. Ferromagnetism has been observed for $x = 0$–0.21. The Curie temperature declines monotonically as the V concentration increases. Single-crystalline samples could only be grown for x values up to 0.21 for which the transition temperature was suppressed down to 36 K. Although we could not fully suppress T_C via V substitution, for $x = 0.16$, we performed magnetization measurements under pressure. The ferromagnetic state is suppressed under pressure at an initial rate of $dT_C/dp \simeq -11.7$ K/GPa and vanishes by 3.3 GPa. The increase of the Rhodes-Wohlfarth ratio suggests that the ferromagnetism in this system evolves toward itinerant as the V concentration increases.

DOI: 10.1103/PhysRevB.88.094405 PACS number(s): 75.30.Cr, 75.50.Cc, 75.30.Gw, 75.30.Kz

I. INTRODUCTION

Transition metals and their compounds can manifest itinerant magnetic behavior, with their magnetic properties originating from delocalized d electrons.[1–3] Unlike the localized $4f$ electrons in the lanthanide series or the multiconfigurational $5f$ electrons in some of the actinide elements,[4,5] the d electrons' orbitals can be significantly altered by the formation of chemical bonds. The d electrons often become part of the conduction band, propagating in the materials; thus, their wave functions are very different from those of localized electrons. This gives rise to the relatively large exchange interactions between the d electrons. Based on the Stoner criterion,[6] at a critical value of the density of states (DOS) and on-site repulsion, d electrons can spontaneously split into spin-up and spin-down subbands, which leads to ferromagnetic ordering. Although the Stoner theory[6] provides the grounds for understanding the itinerant ferromagnetic state, there are still questions left to be answered about the role of spin fluctuations and the quantum criticality in the itinerant ferromagnetic systems.

Itinerant ferromagnets are of particular interest for studying the mechanism of magnetism and superconductivity near a quantum critical point (QCP). Unlike the classical phase transitions driven by temperature, a quantum phase transition (QPT) at zero temperature is driven by nonthermal parameters.[7] A QCP is thought to be a singularity in the ground state, at which point the characteristic energy scale of fluctuations above the ground state vanishes.[7] In itinerant ferromagnets, the temperature dependence of the magnetic properties has often been interpreted in terms of spin fluctuations.[8–10] With the spin fluctuations, an ordered ground state can change into a nonordered state by crossing a QCP. Non-Fermi-liquid behaviors of the materials associated with a QCP can often be observed, such as the temperature divergences of the physical properties.[11–16] Moreover, superconductivity has been discovered in the vicinity of a QCP in weakly ferromagnetic systems, such as in the case of UGe_2 (Refs. 17–19) and UCoGe.[20] On the boundary of a ferromagnetic state at low temperatures, a strong longitudinal magnetic susceptibility and magnetic interactions may lead to a superconducting state.[18,21,22] The parallel-spin quasiparticles in the ferromagnetic system should form pairs in odd-parity orbitals, based on the Pauli exclusion principle. Theories suggest that this type of superconductivity should be spin triplet and magnetically mediated.[18,21,22] Thus, the suppression of ferromagnetism and the search for a QCP in the itinerant ferromagnetic systems may offer a better understanding of the magnetically mediated superconductivity and non-Fermi-liquid behaviors. Chemical doping, pressure, and magnetic field are often used to tune the magnetic orderings and drive the criticality. For example, a QCP emerges in $Zr_{1-x}Nb_xZn_2$ when the doping level reaches $x_c = 0.083$,[23] and in $CePd_{1-x}Ni_x$ when the doping level is 0.95.[12] YbAgGe,[14] YbPtBi,[16] and $YbRh_2Si_2$ (Ref. 24) can be driven to field-induced QCPs associated with a non-Fermi-liquid behavior in the resistivity. In the case of MnSi (Ref. 3) and UGe_2,[17] itinerant-electron magnetism disappears at a first-order transition and a QPT appears as pressure is applied.

Both $LaCrGe_3$ and $LaVGe_3$ were reported to form in a hexagonal perovskite-type (space group $P6_3/mmc$) structure.[25,26] The structure consists of chains of face-sharing Cr-centered (or V-centered) octahedra extended along the c direction. The short Cr-Cr (or V-V) distances have been taken as an indication of weak metal-metal bonding.[25,26] It is suggested that by applying the conventional geometric arguments for stabilizing perovskite-related structures, the hexagonal form is favored over the more common cubic form with the Goldschmidt tolerance factor $t > 1$.[26,27] Whereas $LaVGe_3$ is found to be nonmagnetic above 2 K,[26] $LaCrGe_3$ was reported to order ferromagnetically at 78 K.[25,28] Previous work suggests $LaCrGe_3$ is an itinerant ferromagnet, with an estimated effective moment, 1.4 μ_B/f.u., that is significantly lower than the expected values of Cr^{4+} (2.8 μ_B) or Cr^{3+} (3.8 μ_B).[26] Based on the band structure calculated for both compounds, it is claimed that they have very similar DOS features and can probably be explained by the rigid-band model.[25,26] For $LaCrGe_3$, the d state of Cr manifests as a sharp peak near the Fermi level in the DOS, consistent with itinerant ferromagnetism as suggested by the Stoner model.[6] $LaVGe_3$,

with fewer electrons, fills the band up to a lower energy level. Thus, the Fermi level of $LaVGe_3$ lies at a local minimum of the DOS and shows paramagnetic behavior.

To suppress the ferromagnetism in this system, substituting V for Cr in $LaV_xCr_{1-x}Ge_3$ is one of the rational choices, since this is expected to tune the DOS by changing the position of the Fermi level. Studies of polycrystalline samples show that V substitution does change the magnetic exchange interactions, and the long-range magnetic ordering is suppressed.[26] Only the temperature dependence of magnetization was measured on the polycrystalline samples and the precise stoichiometry of this doped system was not analyzed by chemical or physical measurement. The V-concentration dependence of Curie temperature was not reported and it is not clear at which concentration the ferromagnetism is fully suppressed. Detailed measurements of transport and thermodynamic properties of the doped system are needed, in the hope that they will allow one to follow the evolution of the ferromagnetism and distinguish between itinerant and local-moment magnetism.

Besides chemical substitution, an itinerant magnetic system can often be perturbed by applying pressure. Thus, for the $LaV_xCr_{1-x}Ge_3$ series, pressure can also be used to suppress the magnetic state and discover a possible QCP.

In this work, we report the synthesis of single-crystalline $LaV_xCr_{1-x}Ge_3$ ($x = 0$–0.21, 1.00) samples and present a systematic study of their transport and thermodynamic properties. A ferromagnetic transition has been confirmed. Both the effective moment and the saturated moment per Cr decrease systematically as V concentration increases, with the saturated moment decreasing much more rapidly, indicating that the Cr moment is fragile. The associated increase of the Rhodes-Wohlfarth ratio suggests that the ferromagnetism in this system becomes more and more itinerant as x increases. The Curie temperature decreases with V substitution. The magnetic ordering is suppressed down to 36 K for the highest level of V substitution obtained ($x = 0.21$), other than the nonmagnetic $LaVGe_3$. Given that ferromagnetism is not completely suppressed by our highest level of V substitution, measurements of magnetization under pressure were performed on the $x = 0.16$ sample. The ferromagnetic state is suppressed by the increasing pressure and vanishes by 3.3 GPa.

II. EXPERIMENTAL DETAILS

The relatively deep eutectic in the Cr-Ge binary[29] provides an opportunity to grow $LaV_xCr_{1-x}Ge_3$ compounds out of high-temperature solutions.[30,31] Single crystals of $LaV_xCr_{1-x}Ge_3$ were synthesized with a ratio of $La : V : Cr : Ge = (13 + 2x) : 10x : (13 - 13x) : (74 + x)$ ($0 \leqslant x \leqslant 0.6$). High purity ($>3N$) elements La, V, Cr, and Ge were premixed by arc melting. The ingot was then loaded into a 2 ml alumina crucible and sealed in a fused silica tube under a partial pressure of high-purity argon gas. The ampoule containing the growth materials was heated up to 1100 °C over 3 h and held at 1100 °C for another 3 h. The growth was then cooled to 825 °C over 65 h at which temperature the excess liquid was decanted using a centrifuge.[30,31] For $x = 1.0$, i.e., $LaVGe_3$, excess Ge flux was used with an initial composition of $La : V : Ge = 15 : 10 : 75$, and the decanting temperature was adjusted to

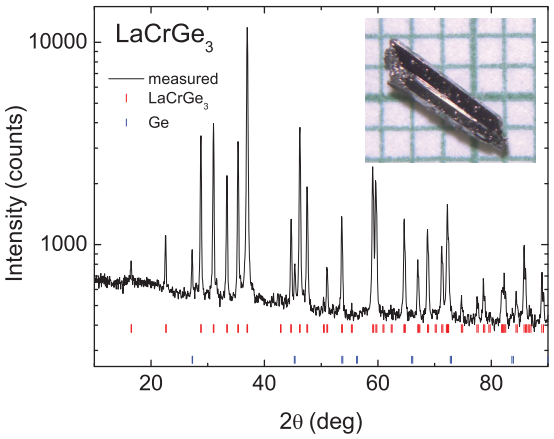

FIG. 1. (Color online) Powder x-ray diffraction pattern of $LaCrGe_3$. Inset: Photo of a single-crystalline $LaCrGe_3$ sample on a millimeter grid.

880 °C accordingly. Single crystals of $LaV_xCr_{1-x}Ge_3$ grew as hexagonal rods with typical size of $\sim 0.7 \times 0.7 \times 5\ mm^3$ (seen in the inset of Fig. 1). A considerable amount of second phase material was grown as the result of secondary solidification, which was identified to be $V_{11}Ge_8$ by powder x-ray diffraction. For growths with initial composition of $0.6 < x < 1.0$, the sizes of crystals dramatically decreased to submillimeters and could not be visually distinguished from the secondary solidification ($V_{11}Ge_8$). Despite multiple attempts, single-crystalline $LaV_xCr_{1-x}Ge_3$ samples with higher x, which are distinguishable from the secondary solidification, could not be grown.

Powder x-ray diffraction data were collected on a Rigaku MiniFlex II diffractometer with Cu Kα radiation at room temperature. Samples with rodlike shape were selected for the measurement. Data collection was performed with a counting time of 2 s for every 0.02 degree. The LeBail refinement was conducted using the program RIETICA.[32] Error bars associated with the values of the lattice parameters were determined by statistical errors, and Si powder standard was used as an internal reference.

Elemental analysis of the samples was performed using wavelength-dispersive x-ray spectroscopy (WDS) in a JEOL JXA-8200 electron probe microanalyzer. Only clear and shiny as-grown surface regions were selected for determination of the sample stoichiometry, i.e., regions with residual Ge flux were avoided. For each compound, the WDS data were collected from multiple points on the same sample.

The ac resistivity was measured by a standard four-probe method in a Quantum Design, Physical Property Measurement System (PPMS). Platinum wires were attached to the sample using Epo-tek H20E silver epoxy, with the current flowing along the c axis. The absolute values of resistivity are accurate to $\pm 15\%$ due to the accuracy of measurements of the electrical contacts' positions.

Measurements of field- and temperature-dependent magnetization were performed in a Quantum Design, Magnetic Property Measurement System (MPMS). Magnetization measurements were made by mounting the single-crystal samples in a pair of transparent plastic straws. For the applied field $\mathbf{H} \parallel c$, the crystal was placed between the outer diameter of

the inner straw and the inner diameter of the outer straw, with both being completely uniform along their lengths. In this field direction, there was no addenda associated with the sample mounting. For the applied field $\mathbf{H} \parallel ab$, the crystal was placed between two halves of the split inner straw with a <2 cm^2 of transparent plastic film covering the two open ends, providing an effective support for the crystal. The addendum associated with this mounting was less than $\sim$10% of our smallest signal at the highest temperature. The effective moments calculated for $\mathbf{H} \parallel c$, $\mathbf{H} \parallel ab$ and for an effective polycrystalline average [$\chi_{\text{ave}} = \frac{1}{3}\ (\chi_c + 2\chi_{ab})$] are all within 0.1 μ_B/Cr of each other, demonstrating basic isotropy of the high-temperature, paramagnetic state of these samples. For this work, we will use the results of the polycrystalline average data.

Temperature-dependent specific heat in zero field was measured in a PPMS using the relaxation technique for representative samples. The specific heat of $LaVGe_3$ was used to estimate the nonmagnetic contributions to the specific heat of $LaV_xCr_{1-x}Ge_3$. The magnetic contribution to specific heat from the Cr ions was calculated by the relation $C_M = C_p(LaV_xCr_{1-x}Ge_3) - C_p(LaVGe_3)$.

The temperature-dependent, field-cooled magnetization of a single crystal for $x = 0.16$ under pressure was measured in a Quantum Design MPMS superconducting quantum interference device (SQUID) magnetometer in a magnetic field of 20 Oe, 50 Oe, and 1 kOe applied along the c axis. Pressures of up to 4.9 GPa were achieved with a moissanite anvil cell.[33] The body of the cell is made of Cu-Ti alloy and the gasket is made of Cu-Be. Daphne 7474 was used as a pressure-transmitting medium, and the pressure was determined at 77 K by the ruby fluorescence technique.

III. RESULTS AND ANALYSIS

A. Crystal stoichiometry and structure

The stoichiometry of the $LaV_xCr_{1-x}Ge_3$ samples was inferred by WDS analysis. Table I summarizes the normalized results showing the atomic percent of each element. The ratio of La : (V + Cr) : Ge stays roughly as 1:1:3. The variation is induced by systematic error, and the counting statistics suggests that there should be 2% or less relative error due to counting. As shown in the inset of Fig. 2, the ratio of x_{WDS} over x_{nominal} is approximately 0.4, and the small 2σ values

TABLE I. The WDS data (in atomic %) for $LaV_xCr_{1-x}Ge_3$. N is the number of points measured on one sample, x_{nominal} is the nominal concentration, x_{WDS} is the average x value measured, and 2σ is two times the standard deviation of x_{WDS} from the N values measured. Note: the variation is induced by systematic error, and the counting statistics suggests 2% or less relative error due to counting.

x_{nominal}	N	La	V	Cr	Ge	x_{WDS}	2σ
0.00	13	20.06	0.01	19.80	60.13	0.00	0
0.08	14	20.00	0.83	18.74	60.42	0.04	0.01
0.25	12	19.98	1.76	17.89	60.36	0.09	0.01
0.34	12	20.01	3.06	16.50	60.43	0.16	0.01
0.43	16	20.04	3.69	16.09	60.19	0.19	0.02
0.54	12	20.41	4.29	15.75	59.49	0.21	0.01
1.00	14	19.66	20.46	0.09	59.79	1.00	0.01

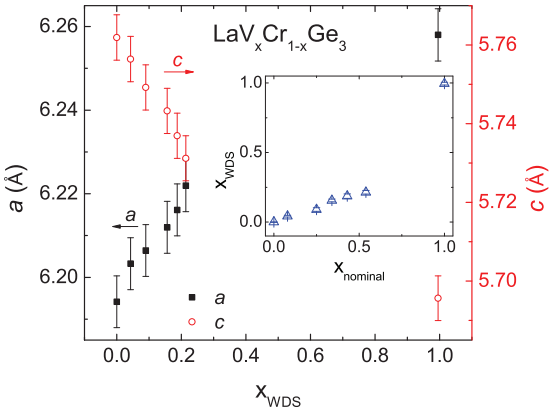

FIG. 2. (Color online) The lattice parameters a and c of single-crystalline $LaV_xCr_{1-x}Ge_3$ compounds vs V concentration x_{WDS} measured by WDS. Inset: x_{WDS} vs x_{nominal}.

suggest that the samples are homogeneous. In the following, the measured (x_{WDS}) rather than nominal x values will be used to index the stoichiometry of the compounds in this series.

Powder x-ray diffraction patterns were collected on ground single crystals from each compound. Figure 1 presents the $LaCrGe_3$ x-ray pattern as an example. The main phase was refined with the known $P6_3/mmc$ (No. 194) structure. Small traces of Ge residue can be detected, whereas no clear evidence of La-Ge, V-Ge, or Cr-Ge binaries was found. Similar results ($P6_3/mmc$ structure with minority phase of Ge) were obtained for the rest of the series. The lattice parameters, obtained by the analysis of the powder x-ray diffraction data, are presented in Fig. 2. As is shown, a and c are monotonically changing as the x increases, which is consistent with the reported data.[26] Crystallographically, transition-metal elements in $LaCrGe_3$ and $LaVGe_3$ occupy the same unique site $2a$.[25,26]

B. Effects of chemical substitution on the physical properties of $LaV_xCr_{1-x}Ge_3$

Figures 3(a)–3(f) present the anisotropic field-dependent magnetization isotherms for the $LaV_xCr_{1-x}Ge_3$ ($x = 0$–0.21) series. The measurements were performed with $\mathbf{H}$ parallel to the ab plane and the c axis at 2 K. For $\mathbf{H} \parallel c$, the magnetization of all compounds saturates very rapidly as the magnetic field increases from $H = 0$, which is a manifestation of a typical ferromagnetic behavior. For $\mathbf{H} \parallel ab$, the magnetization rises more slowly as the applied field increases. As can be seen, in low fields, $M_c \gg M_{ab}$; at $H = H_{\text{Equal}}$, M_c equals M_{ab}; and in high fields, $M_c < M_{ab}$. Also, as x increases, H_{Equal} decreases monotonically, as shown in Fig. 4. We identify the c axis as the easy axis in low fields, and the x dependence of H_{Equal} presents a calliper of the diminishing range of the low-field $M_c > M_{ab}$ anisotropy. These data suggest that the $LaV_xCr_{1-x}Ge_3$ compounds may have a complex magnetic structure with a ferromagnetic component along the c axis. The change of anisotropy is probably caused by field-induced spin reorientation, which is consistent with the previous neutron study.[28] For $\mathbf{H} \parallel c$, the saturated moment μ_S per Cr is determined by linear extrapolations of the magnetization from high fields to $H = 0$. For $x = 0$, μ_S is found to be about 1.25 μ_B/Cr, essentially identical to the reported value 1.22 μ_B.[28] It

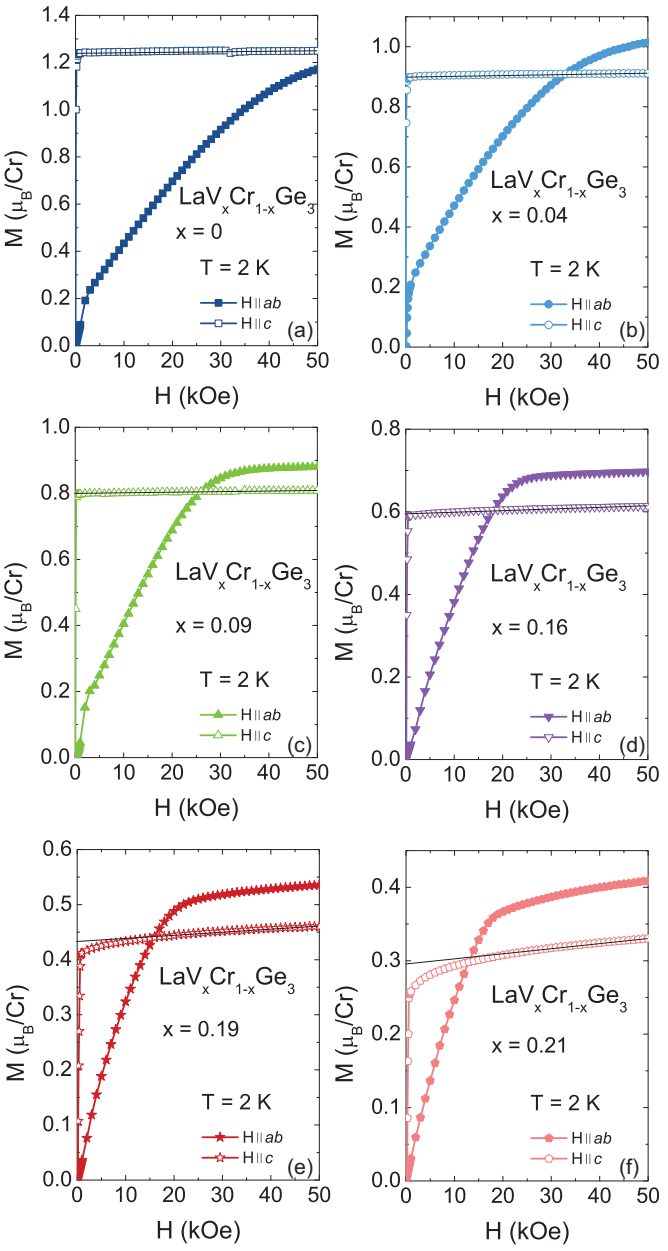

FIG. 3. (Color online) Anisotropic field-dependent magnetization data for $LaV_xCr_{1-x}Ge_3$ ($x = 0$–0.21) taken at 2 K. Fine solid lines through the high-field $\mathbf{H} \parallel c$ data extrapolate back to $H = 0$, μ_S values shown in Table II.

monotonically decreases as the V concentration increases and drops to 0.30 μ_B/Cr for $x = 0.21$. The values of the saturated moment μ_S with $\mathbf{H} \parallel c$ are summarized in Table II. Again, the decrease of the saturated moment implies that the $LaV_xCr_{1-x}Ge_3$ series probably is an itinerant ferromagnetic system.[25]

To estimate the Curie temperature T_C from the magnetization measurements, we studied the temperature-dependent, field-cooled (FC) magnetization of the $LaV_xCr_{1-x}Ge_3$ series, with $\mathbf{H} \parallel c$ at 50 Oe, as shown in Fig. 5. The magnetization for $LaCrGe_3$ exhibits a sudden increase near 90 K, indicating a transition to a ferromagnetic state. However, at around 68 K, its value starts declining, then saturates at low temperatures,

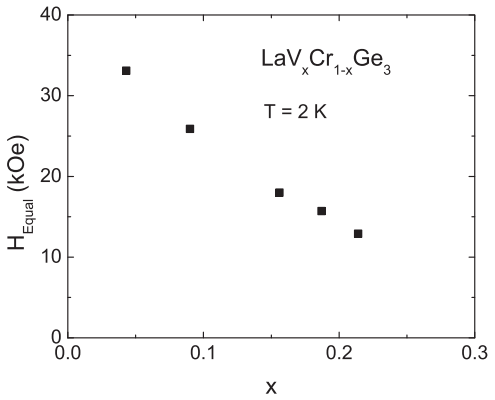

FIG. 4. H_{Equal} (the field at which $M_c = M_{ab}$) as a function of x for $LaV_xCr_{1-x}Ge_3$ ($x = 0.04$–0.21) taken at 2 K.

leaving a peak seen in its magnetization. This is probably associated with the changes of the magnetic domains and the demagnetization field upon cooling. A similar feature was not observed for the V-doped compounds. It is possibly due to the pinning effect brought by the V substitution. For the other members of the series, the susceptibility shows the expected, rapid increase and the tendency to saturation at low temperatures, which indicate the existence of a ferromagnetic state in this series for x up to 0.21. The Curie temperature was estimated by extrapolating the maximum slope in M/H to zero, as shown by the arrow in the inset of Fig. 5; the T_C values are listed in Table II. Given that these are very-low-field $M(T)$ data, these values should not be too different from those inferred from the Arrott plots; see Fig. 6. The monotonic change of the Curie temperature demonstrates that the ferromagnetism in the $LaV_xCr_{1-x}Ge_3$ series is systematically suppressed by the V substitution.

Given that a ferromagnet possesses a spontaneous magnetization below its Curie temperature, even without external magnetic field applied, the determination of the Curie temperature from the temperature-dependent magnetization is not without ambiguity. To better evaluate the Curie temperature, magnetization isotherms in the vicinity of T_C were measured for $x = 0.16$ [Fig. 6(a)]. Since the ferromagnetic component is believed to be along the c axis, the magnetic field was applied along the c axis. In addition, in this orientation, we also reduce

TABLE II. Summarized μ_S ($\mathbf{H} \parallel c$), μ_{eff}, θ, and ordering temperatures from magnetization T_C^{mag}, resistivity T_C^{ρ}, specific heat $T_C^{C_p}$, Arrott plot data, and residual resistivity ρ_0 for $LaV_xCr_{1-x}Ge_3$ ($x = 0$–0.21).

x_{WDS}	μ_S, $\mathbf{H} \parallel c$ (μ_B/Cr)	μ_{eff} (μ_B/Cr)	θ (K)	T_C^{mag} (K)	T_C^{ρ} (K)	$T_C^{C_p}$ (K)	T_C (Arrott) (K)	ρ_0 ($\mu\Omega$ cm)
0.00	1.25	2.5	91.7	88	84	85		36
0.04	0.91	2.3	84.7	73	68	69		78
0.09	0.81	2.2	64.6	61	54	62		116
0.16	0.59	2.1	45.9	52	37	46	50 ± 1	100
0.19	0.43	2.0	26.2	46				97
0.21	0.30	1.9	6.7	36				66
1.00								8

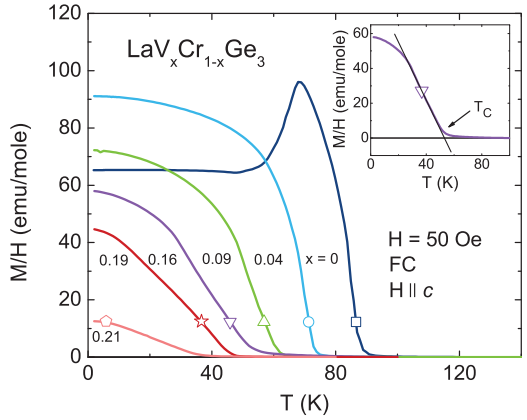

FIG. 5. (Color online) Field-cooled (FC) magnetization as a function of temperature for $LaV_xCr_{1-x}Ge_3$ ($x = 0$–0.21) at 50 Oe with $\mathbf{H} \parallel c$. Inset: Enlarged temperature dependence of magnetization near phase transition for $x = 0.16$. The arrow shows the criterion used to infer the transition temperature.

the uncertainty caused by the demagnetization signal along the long axis of the rodlike sample.

As can be seen in Fig. 6(a), spontaneous magnetization can be easily observed for $M(H)$ measured at 43, 46, 48, and 49 K, indicating that the system possesses a state with a ferromagnetic component at least up to 49 K. To further refine our determination of the Curie temperature, an Arrott plot for $x = 0.16$ is presented in Fig. 6(b). According to Arrott,[34] at T_C, the relation between the magnetic field H and the magnetization M can be written in the form of a power-law expansion:

$$\frac{M_0 H}{N_A k_B T_C} = a_1 \left(\frac{M}{M_0}\right)^3 + a_2 \left(\frac{M}{M_0}\right)^5 + \cdots .$$

Here, a_1 and a_2 are the expansion coefficients, M_0 is the saturated magnetization at zero temperature, and N_A is Avogadro's number. This relation is valid under the condition $M \ll M_0$, i.e., in the low-field region. Therefore, further approximation can be made by only considering the first term in the expansion which leads to the Arrott-Noakes[34,35] relation $(H/M) \propto M^2$ at T_C. It suggests that the ferromagnetic ordering temperature T_C can be inferred from the magnetization data by noting the temperature at which the low-field data pass though the origin. As shown in Fig. 6(b), the Curie temperature for $x = 0.16$ is about 50 ± 1 K, which is very close to the value obtained from the low-field magnetization measurement (also seen in Table II). Therefore, the T_C determined from the low-field magnetization data appears to be reliable for these materials.

The isothermal curves shown in Fig. 6(b) are found to be deviated from the linearity in the Arrott plot. It should be noted that the theoretical justification on the Arrott plot is based on a simple and clearly defined Landau-type second-order phase transition.[34] In the real materials, such deviations can be observed in a disordered system with complex magnetic phenomena and can be affected by many factors, such as the coupling between the homogeneous matrix and the magnetic clusters, domain wall pinning, or even proximity to field stabilized states, etc.[36–38]

The inverse of the polycrystalline averaged susceptibility H/M measured at 1 kOe is shown in Fig. 7. The polycrystalline averaged susceptibility was estimated by $\chi_{ave} = \frac{1}{3}(\chi_c + 2\chi_{ab})$. At high temperatures, all of the compounds follow the Curie-Weiss behavior. It should be mentioned that the susceptibility of $LaVGe_3$ is about three orders of magnitude

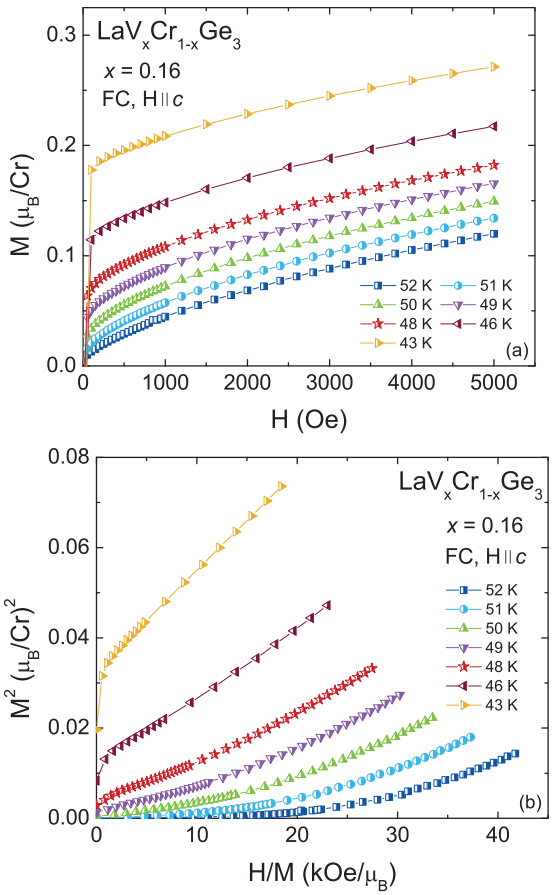

FIG. 6. (Color online) (a) Magnetization isotherms for $x = 0.16$ measured at different temperatures. (b) The Arrott plot in the form of M^2 vs H/M for $x = 0.16$, with $\mathbf{H} \parallel c$.

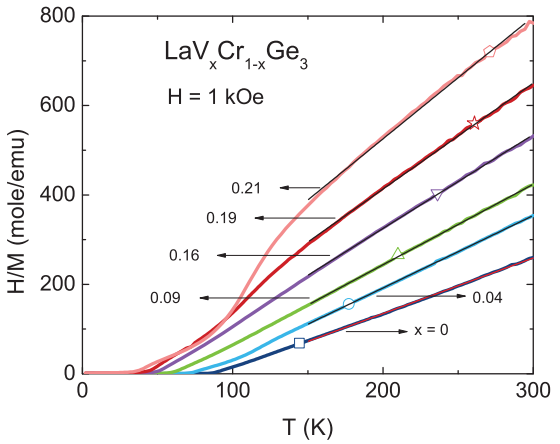

FIG. 7. (Color online) The polycrystalline averaged inverse susceptibility H/M as a function of temperature for $LaV_xCr_{1-x}Ge_3$ ($x = 0$–0.21) measured at $H = 1$ kOe. The data were fitted with $1/\chi = (T - \theta)/C$ as indicated by the solid lines.

smaller than those of $LaV_xCr_{1-x}Ge_3$ ($x = 0$–0.21); thus, its possible Pauli paramagnetic contribution is negligible. On the other hand, evident deviations from the Curie-Weiss law can be observed below 130 K for $x = 0.19$ and 0.21. Further investigations are needed to understand the origin of these deviations. The temperature range of 150 to 300 K was selected for fitting the high-temperature magnetic susceptibility with $1/\chi = (T - \theta)/C$, where θ is the Curie-Weiss temperature and C is the Curie constant. The effective moments μ_{eff} and θ are summarized in Table II. Considering the presence of small amount of Ge and $V_{11}Ge_8$, as well as the accuracy of measuring the sample's mass, the values of μ_{eff} in this series are accurate to ±5%. Shown in Fig. 7, as x increases, μ_{eff} per Cr decreases systematically, the slope of the H/M curve rises gradually, and the Curie-Weiss temperature decreases from 91.7 K for $x = 0$ to 6.7 K for $x = 0.21$ monotonically. The positive θ values indicate that ferromagnetic interactions are dominant in this series. The decrease in θ suggests that the ferromagnetic interaction is suppressed by V doping. Based on all of these results, it is highly likely that the Cr ions in the $LaV_xCr_{1-x}Ge_3$ compounds manifest non-local-moment-like behavior. It should be noted that for $x = 0$, the $\mu_{\text{eff}} = 2.5\ \mu_B$/Cr value we found is significantly larger than the reported value (1.4 μ_B) inferred from the data on polycrystalline samples.[25] Not only is the Ref. 25 value different from our $x = 0$ value, but it is inconsistent with μ_{eff} evolution across the whole series (Fig. 7 and Table II). It is also inconsistent with the μ_{eff} that we measured on polycrystalline samples: $\mu_{\text{eff}} = 2.5\ \mu_B$/Cr for $x = 0.07$ and $\mu_{\text{eff}} = 2.3\ \mu_B$/Cr for $x = 0.13$.

The electrical resistivity as a function of temperature for $LaV_xCr_{1-x}Ge_3$ is presented in Fig. 8(a). At high temperatures, the electrical resistivity drops linearly upon cooling, characteristic of normal-metallic behavior. For $LaCrGe_3$, due to the loss of spin disorder scattering, a clear break in resistivity occurs at about 84 K. With the subtraction of the residual resistivity ρ_0 (listed in Table II), the evolution of the ferromagnetic transition with increasing x can be clearly seen in Fig. 8(b). As the V-doping level increases, the spin disorder scattering associated with the Cr moment ordering becomes broadened. For $x = 0.19$ and 0.21, the feature is too subtle to be clearly detected. Due to the broadening transition feature, determining T_C via $d\rho/dT$ is problematic. Instead,

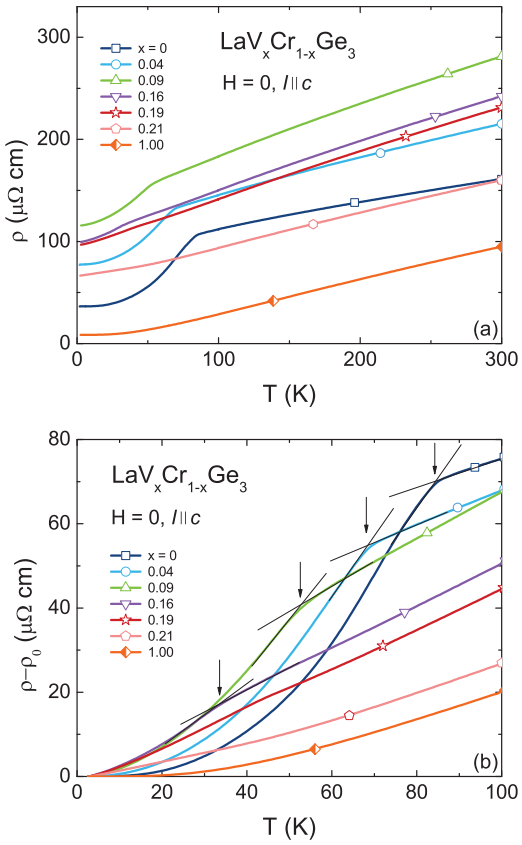

FIG. 8. (Color online) (a) The temperature-dependent electrical resistivity for the $LaV_xCr_{1-x}Ge_3$ compounds. (b) Enlarged temperature-dependent ρ-ρ_0 at low temperatures. The transition temperatures are shown by the arrows.

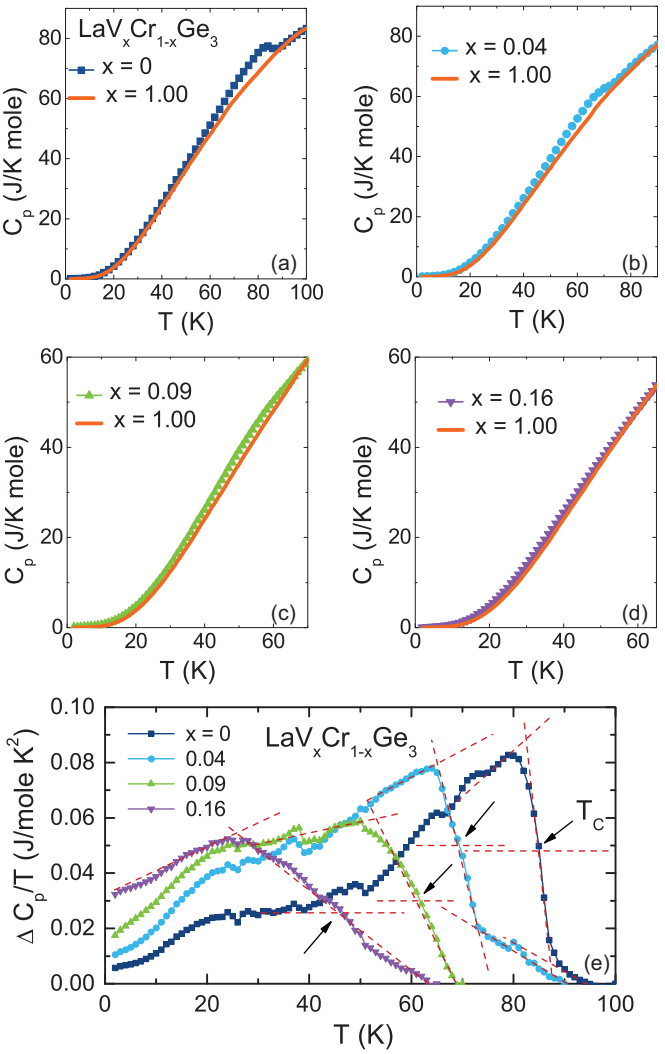

FIG. 9. (Color online) Temperature dependence of specific heat for $LaV_xCr_{1-x}Ge_3$ with (a) $x = 0$ and 1.00, (b) $x = 0.04$ and 1.00, (c) $x = 0.09$ and 1.00, and (d) $x = 0.19$ and 1.00. (e) Magnetic contributions to the specific heat as a function of temperature for $LaV_xCr_{1-x}Ge_3$ ($x = 0$–0.16). The arrows show the criteria used to infer the transition temperature.

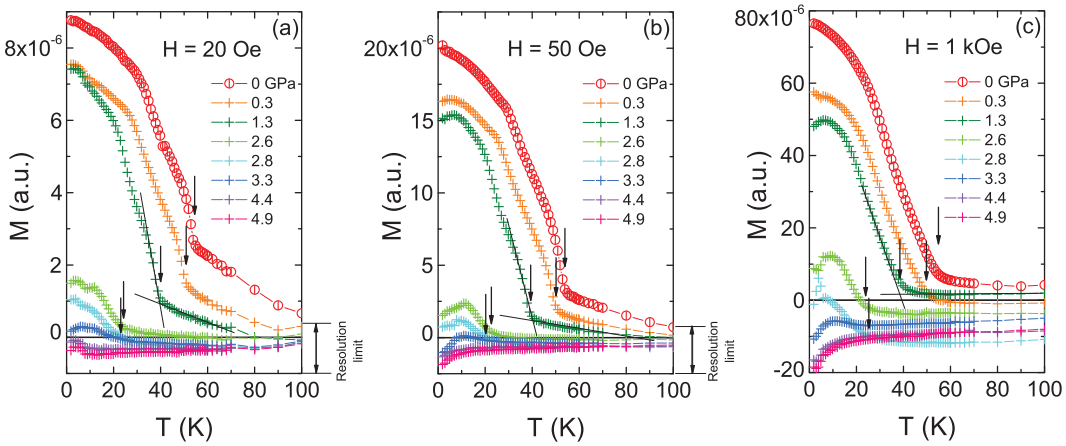

FIG. 10. (Color online) Temperature dependence of the field-cooled magnetization for $x = 0.16$ under different pressures with $\mathbf{H} \parallel c$ at (a) 20 Oe, (b) 50 Oe, and (c) 1 kOe. Arrows indicate the criteria for the determination of the Curie temperature T_C.

the point at which the slope of $\rho(T)$ changes is used to infer the critical temperature in the resistivity data, as indicated by the arrows in Fig. 8(b). The inferred T_C^{ρ} is summarized in Table II, and it is clear that the Curie temperature decreases monotonically as the V concentration increases. In addition, ρ_0 seems to show a broad maximum as x increases, which is likely due to more disorder/impurities induced by substitution. The nonmonotonic behavior of ρ_0 is common for substitution series where $x = 0$ and $x = 1$ are well-ordered, stoichiometric compounds. The broad maximum located closer to the Cr side is not unexpected given that Cr magnetism (and any scattering associated with it) appears to be dramatically suppressed by V substitution.

The temperature-dependent specific-heat data for the $LaV_xCr_{1-x}Ge_3$ ($x = 0$, 0.04, 0.09, 0.16, and 1.00) series are presented in Figs. 9(a)–9(d). The specific heat can be estimated by the relation $C_p(T) = C_e + C_{ph} + C_M$, where C_e is the conduction electron contribution, C_{ph} is the phonon contribution, and C_M is the magnetic contribution. Since $LaVGe_3$ is nonmagnetic, $C_e + C_{ph}$ can be approximated by the C_p data of $LaVGe_3$. Thus, the magnetic contribution C_M can be evaluated by the relation $C_M = C_p(LaV_xCr_{1-x}Ge_3) - C_p(LaVGe_3)$. For a clearer presentation of the transition feature, $C_p(T)$ of all compounds were normalized with respect to the specific heat of $LaVGe_3$, $C_p(LaVGe_3)$, with the highest-temperature C_p values set to be equal [as seen in Figs. 9(a)–9(d)]. The changes induced by the normalization are less than 3%. An anomaly can be observed in the $C_p(LaV_xCr_{1-x}Ge_3)$ with the comparison of $C_p(LaVGe_3)$. This anomaly, associated with the ferromagnetic transition, can be best seen in the $LaCrGe_3$ sample, at ~85 K. As the V-doping level increases, the feature becomes less obvious and systematically shifts to lower temperatures. For $x \geqslant 0.19$, this feature is no longer detectable. To estimate the ordering temperature, $\triangle C_p/T$ for $x = 0$, 0.04, 0.09, and 0.16 are plotted in Fig. 9(e). The magnetic phase transition manifests itself as a local maximum. The change of slope seen at ~87 K for $x = 0$ and ~73 K for $x = 0.04$ may indicate the onset of the transition. The midpoint on the rise of $\triangle C_p/T$ was chosen as the criteria for $T_C^{C_p}$, as indicated by the arrows in the plot. These $T_C^{C_p}$ values are also presented in Table II. Again, we observe that with the increasing amount of V substituted for Cr, the ferromagnetic state in this series is gradually suppressed.

C. Effects of pressure on the magnetic properties of $LaV_xCr_{1-x}Ge_3$

Given that (i) we could only grow single crystals for $x \leqslant 0.21$ and (ii) up to $x = 0.16$, the ferromagnetic transition can be confirmed in different measurements, we decided to evaluate the potential for quantum critical behavior by using pressure as a second tuning parameter. Figures 10(a)–10(c) show the temperature dependence of the field-cooled magnetization for $x = 0.16$ measured under different pressures. The measurements were performed with $\mathbf{H} \parallel c$ and $H = 20$ Oe, 50 Oe, and 1 kOe. The Curie temperature T_C is revealed by a rather sharp increase of the magnetization. Due to the loss of the signal, there is a serious limitation to the determination of T_C close to the critical pressure. For higher field, $H = 1$ kOe [Fig. 10(c)], measurements and data analysis are limited to the large background of the pressure cell (this is the most likely source of apparent diamagnetic shifts in higher-pressure data). By comparing Figs. 10(a)–10(c), the magnetization under

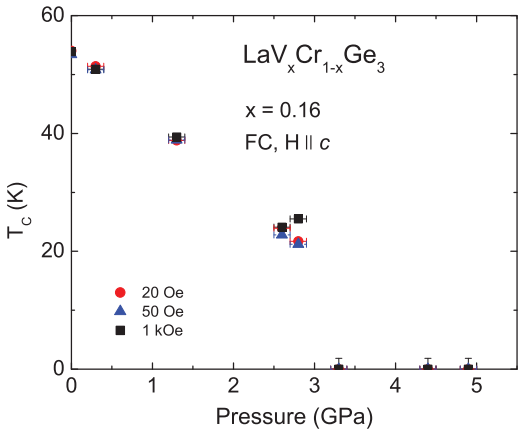

FIG. 11. (Color online) Pressure dependence of T_C for $x = 0.16$ measured at 20 Oe, 50 Oe, and 1 kOe.

3.3 GPa is not considered as a ferromagnetic behavior. The pressure dependences of the Curie temperature measured at different fields show consistent behaviors, as plotted in Fig. 11. The result shows T_C decreases with applied pressure at an initial rate of $dT_C/dp \simeq -11.7$ K/GPa below 2.8 GPa, and no ferromagnetic transition can be detected in our measurements above 3.3 GPa. Similarly, the low-temperature magnetization decreases as T_C decreases with applied pressure, as shown in Figs. 10(a)–10(c). Although the low-temperature signal is not necessarily equal to the saturation magnetization, the decrease of the low-temperature magnetization following the decrease of T_C is expected for an itinerant ferromagnet[39] and was experimentally observed in $ZrZn_2$.[2,40]

IV. DISCUSSION AND CONCLUSIONS

The growth of single-crystalline $LaV_xCr_{1-x}Ge_3$ (x = 0–0.21, 1.00) samples has allowed for the detailed study of the anisotropic properties, the determination of the easy axis, and the estimate of the effective moment and saturated moment. In addition, careful chemical analysis was performed to determine the precise concentration of this doped system. This offers a clearer understanding of the chemical substitution effect on the suppression of the ferromagnetism in this system, and is also crucial for calculating the saturated and effective moment per Cr ion.

We have been able to suppress the ferromagnetism in the $LaV_xCr_{1-x}Ge_3$ series via chemical substitution. The ordering temperatures inferred from low-field magnetization, resistivity, and specific-heat measurements are summarized in Table II. A phase diagram of the x-dependent T_C for $LaV_xCr_{1-x}Ge_3$ was assembled in Fig. 12. For $x = 0.19$ and 0.21, magnetic transitions can only be detected in $M(T)$, and not in $\rho(T)$ and $C_p(T)$ measurements. We can see that for the $LaV_xCr_{1-x}Ge_3$ series, the ferromagnetic transition temperature is suppressed almost linearly by V doping: $T_C = 88$ K for $x = 0$, and $T_C = 36$ K for $x = 0.21$. Since single-crystalline $LaV_xCr_{1-x}Ge_3$ compounds with $0.21 < x < 1.00$ were not synthesized, the exact concentration x_c at which the ferromagnetism in this series is completely suppressed via V substitution is not determined. Based on the our

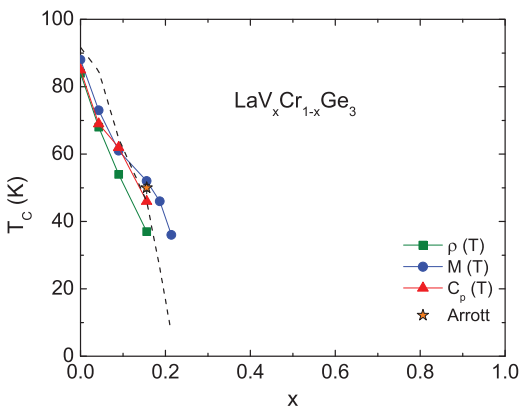

FIG. 12. (Color online) x-dependent T_C for $LaV_xCr_{1-x}Ge_3$ determined by $M(T)$, $\rho(T)$, and $C_p(T)$ measurements, as well as Arrott plot. For comparison, the dashed line indicates the x dependence of the Curie-Weiss temperature, θ, data that is shown in Fig. 13(a).

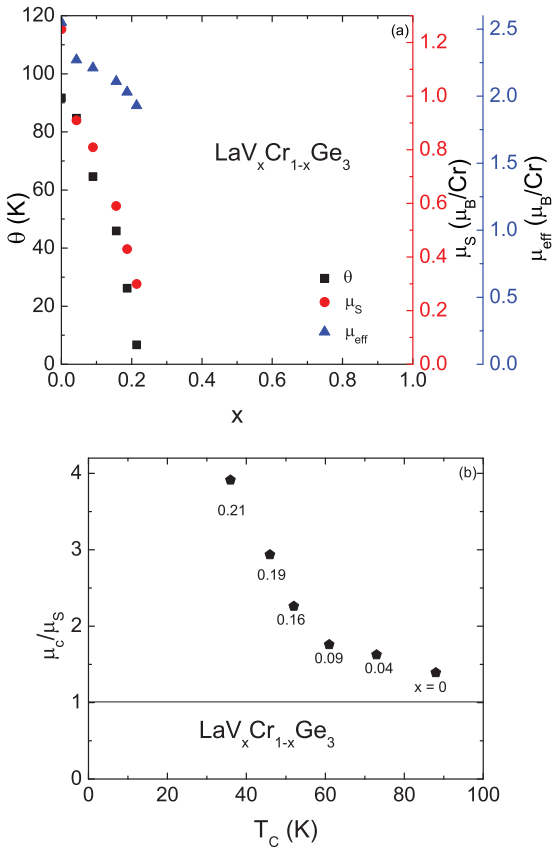

FIG. 13. (Color online) (a) The Curie-Weiss temperature θ, saturated moment μ_S along the c axis, and effective moment μ_{eff} per Cr as a function of x for $LaV_xCr_{1-x}Ge_3$. (b) The Rhodes-Wohlfarth ratio μ_c/μ_S as a function of Curie temperature T_C.

data, a critical concentration is likely to exist near $x = 0.3$. It is worth noting that this is the substitution range in which a linear extrapolation of the H_{Equal} data shown in Fig. 4 reaches zero.

The estimated μ_S and μ_{eff} per Cr as a function of x are plotted in Fig. 13(a). As is shown, both μ_S and μ_{eff} decrease in a clear manner as the V concentration increases. Consistent with the Stoner model, this suggests that the system possesses a fragile ferromagnetism which can be easily perturbed. The criterion for the ferromagnetic state is given by the relation $U\,D(\varepsilon_F) \geqslant 1$, where U and $D(\varepsilon_F)$ are Coulomb repulsion and the DOS at the Fermi level, respectively.[6] Given the fact that T_C decreases as x increases, it is likely that U and/or $D(\varepsilon_F)$ is changed by V substitution in the $LaV_xCr_{1-x}Ge_3$ system. With the increasing level of V doping, the ferromagnetism is continuously suppressed, and will eventually disappear at a critical V concentration x_c. However, due to the lack of higher V-doped samples, x_c cannot be identified precisely in this study. Similarly, in the case of Curie-Weiss temperature, clear suppression in θ by V doping can be observed, as shown in Fig. 13(a). Again, this implies that the ferromagnetic interaction is weakened by V substitution. Given the values of μ_S and μ_{eff}, the Rhodes-Wolfarth ratio (RWR)[41] can be calculated, as seen in Fig. 13(b). According to Rhodes and Wolfarth, RWR $= \mu_c/\mu_S$, where μ_c is related to the number of moment carriers and can be obtained from $\mu_c(\mu_c + 1) = \mu_{eff}^2$. While RWR = 1 is an indication of localized magnetism,

larger RWR values suggest the existence of itinerant ferromagnetism. In our case, for $x = 0$, RWR $\simeq 1.4$, slightly larger than 1, indicating the possibility of the itinerant ferromagnetism. As x increases, RWR increases accordingly, and reaches $\simeq$3.9 for $x = 0.21$, which is much larger than the RWR = 1 criterion. Therefore, it is clear that the ferromagnetism in this series evolves towards itinerant as the V concentration increases. In addition, as x increases, the change of RWR as a function of T_C exhibits very similar behavior as seen in the original Rhodes-Wohlfarth plot.[41] It should be noted that the suppression of ferromagnetism does not necessarily lead to a QPT, and a new magnetic state, such as spin glass, may also emerge.[1,42] However, in the case of the $LaV_xCr_{1-x}Ge_3$ series, given the RWR ratio and the fact that both μ_S and μ_{eff} decrease as the V concentration increases, it is promising that it may be a potential QCP system.[23,41]

We further suppressed the ferromagnetism for $x = 0.16$ by pressure up to 4.9 GPa. As seen in Fig. 11, the Curie temperature decreases as the applied pressure increases, at an initial rate of $dT_C/dp \simeq -11.7$ K/GPa below 2.8 GPa. The ferromagnetic signal vanishes at $\simeq$3.3 GPa and the ferromagnetism in $x = 0.16$ appears to be completely suppressed. Our data clearly show that this system can be brought to a QPT and, hopefully, a QCP. It will be very interesting to study the compounds via transport measurements under pressure and evaluate their critical exponents at p_c. In addition, alternative methods of growing higher x compounds or pressure studies on pure $LaCrGe_3$ will be possible ways to tune the potential QCP system as well.

ACKNOWLEDGMENTS

We thank W. E. Straszheim for his assistance with the elemental analysis of the samples. This work was carried out at Iowa State University and supported by the AFOSR-MURI Grant No. FA9550-09-1-0603 (X.L., V.T., and P.C.). S.B. was supported by the U.S. Department of Energy, Office of Basic Energy Science, Division of Materials Sciences and Engineering. Part of this work was performed at Ames Laboratory, U.S. Department of Energy under Contract No. DE-AC02-07CH11358. X.L. and P.C. also acknowledge H. Miyazaki for key inspiration.

[1] *Magnetism: Fundamentals*, edited by É. du Trémolet de Lacheisserie, D. Gignoux, and M. Schlenker (Springer, Boston, 2005).
[2] M. Uhlarz, C. Pfleiderer, and S. M. Hayden, Phys. Rev. Lett. **93**, 256404 (2004).
[3] C. Thessieu, J. Flouquet, G. Lapertot, A. N. Stepanov, and D. Jaccard, Solid State Comm. **95**, 707 (1995).
[4] C. H. Booth, Y. Jiang, D. L. Wang, J. N. Mitchell, P. H. Tobash, E. D. Bauer, M. A. Wall, P. G. Allen, D. Sokaras, D. Nordlund, T.-C. Weng, M. A. Torrez, and J. L. Sarrao, Proc. Natl. Acad. Sci. USA **109**, 10205 (2012).
[5] R. Troć, Z. Gajek, and A. Pikul, Phys. Rev. B **86**, 224403 (2012).
[6] E. C. Stoner, Phil. Mag. **15**, 1018 (1933).
[7] S. Sachdev, *Quantum Phase Transitions* (Cambridge University Press, Cambridge, UK, 1999).
[8] G. G. Lonzarich, J. Magn. Magn. Mater. **54**, 612 (1986).
[9] G. G. Lonzarich, J. Magn. Magn. Mater. **76**, 1 (1988).
[10] J. Hertz, Phys. Rev. B **14**, 1165 (1976).
[11] G. R. Stewart, Rev. Mod. Phys. **56**, 755 (1984).
[12] G. R. Stewart, Rev. Mod. Phys. **73**, 797 (2001).
[13] G. R. Stewart, Rev. Mod. Phys. **78**, 743 (2006).
[14] S. L. Bud'ko, E. Morosan, and P. C. Canfield, Phys. Rev. B **69**, 014415 (2004).
[15] S. L. Bud'ko, E. Morosan, and P. C. Canfield, Phys. Rev. B **71**, 054408 (2005).
[16] E. D. Mun, S. L. Bud'ko, C. Martin, H. Kim, M. A. Tanatar, J.-H. Park, T. Murphy, G. M. Schmiedeshoff, N. Dilley, R. Prozorov, and P. C. Canfield, Phys. Rev. B **87**, 075120 (2013).
[17] V. Taufour, D. Aoki, G. Knebel, and J. Flouquet, Phys. Rev. Lett. **105**, 217201 (2010).
[18] S. S. Saxena, P. Agarwal, K. Ahilan, F. M. Grosche, R. K. W. Hasselwimmer, M. J. Steiner, E. Pugh, I. R. Walker, S. R. Julian, P. Monthoux, G. G. Lonzarich, A. Huxley, I. Sheikin, D. Braithwaite, and J. Flouquet, Nature (London) **406**, 587 (2000).
[19] A. Huxley, I. Sheikin, E. Ressouche, N. Kernavanois, D. Braithwaite, R. Calemczuk, and J. Flouquet, Phys. Rev. B **63**, 144519 (2001).
[20] N. T. Huy, A. Gasparini, D. E. de Nijs, Y. Huang, J. C. P. Klaasse, T. Gortenmulder, A. de Visser, A. Hamann, T. Görlach, and H. v. Löhneysen, Phys. Rev. Lett. **99**, 067006 (2007).
[21] D. Fay and J. Appel, Phys. Rev. B **22**, 3173 (1980).
[22] K. Miyake, S. Schmitt-Rink, and C. M. Varma, Phys. Rev. B **34**, 6554 (1986).
[23] D. A. Sokolov, M. C. Aronson, W. Gannon, and Z. Fisk, Phys. Rev. Lett. **96**, 116404 (2006).
[24] O. Trovarelli, C. Geibel, S. Mederle, C. Langhammer, F. M. Grosche, P. Gegenwart, M. Lang, G. Sparn, and F. Steglich, Phys. Rev. Lett. **85**, 626 (2000).
[25] H. Bie, O. Y. Zelinska, A. V. Tkachuk, and A. Mar, Chem. Mater. **19**, 4613 (2007).
[26] H. Bie and A. Mar, J. Mater. Chem. **19**, 6225 (2009).
[27] V. M. Goldschmidt, Die Naturwissenschaften **21**, 477 (1926).
[28] J. M. Cadogan, P. Lemoine, B. R. Slater, A. Mar, and M. Avdeev, Solid State Phenom. **194**, 71 (2013).
[29] T. B. Massalski, *Binary Alloy Phase Diagrams*, 2nd ed. (ASM International, New York, 1990).
[30] P. C. Canfield and Z. Fisk, Philos. Mag. B **65**, 1117 (1992).
[31] P. C. Canfield, in *Properties and Applications of Complex Intermetallics*, edited by E. Belin-Ferré (World Scientific, Singapore, 2010).
[32] C. J. Howard and B. A. Hunter, *A Computer Program for Rietveld Analysis of X-Ray and Neutron Powder Diffraction Patterns* (Lucas Heights Research Laboratories, New South Wales, Australia, 1998).
[33] P. L. Alireza, S. Barakat, A. M. Cumberlidge, G. Lonzarich, F. Nakamura, and Y. Maeno, J. Phys. Soc. Jpn. **76SA**, 216 (2007).
[34] A. Arrott, Phys. Rev. **108**, 1394 (1957).

[35] A. Arrott and J. E. Noakes, Phys. Rev. Lett. **19**, 786 (1967).
[36] I. Yeung, R. M. Roshko, and G. Williams, Phys. Rev. B **34**, 3456 (1986).
[37] G. Hilscher, J. Magn. Magn. Mater. **25**, 229 (1982).
[38] S. Jia, N. Ni, G. D. Samolyuk, A. Safa-Sefat, K. Dennis, H. Ko, G. J. Miller, S. L. Bud'ko, and P. C. Canfield, Phys. Rev. B **77**, 104408 (2008).
[39] T. Moriya and A. Kawabata, J. Phys. Soc. Jpn. **35**, 669 (1973).
[40] J. G. Huber, M. B. Maple, D. Wohlleben, and G. S. Knapp, Solid State Comm. **16**, 211 (1975).
[41] P. Rhodes and E. P. Wohlfarth, Proc. R. Soc. London Ser. A **273**, 247 (1963).
[42] J. A. Mydosh, *Spin Glasses: An Experimental Introduction* (Taylor and Francis, London, 1993).